Title

The Interaction between ORF18 and ORF30 Is Required for Late Gene Expression in Kaposi's Sarcoma-Associated Herpesvirus

Journal

Journal of Virology, 93(1)

ISSN

0022-538X

Authors

Castaneda, Angelica F

Glaunsinger, Britt A

Publication Date

2019

DOI

10.1128/jvi.01488-18

Peer reviewed

AMERICAN SOCIETY FOR MICROBIOLOGY | Journal of Virology®

The Interaction between ORF18 and ORF30 Is Required for Late Gene Expression in Kaposi's Sarcoma-Associated Herpesvirus

Angelica F. Castañeda,[a] Britt A. Glaunsinger[a,b]

[a]Department of Plant and Microbial Biology, University of California, Berkeley, Berkeley, California, USA
[b]Howard Hughes Medical Institute, Berkeley, California, USA

ABSTRACT In the beta- and gammaherpesviruses, a specialized complex of viral transcriptional activators (vTAs) coordinate to direct expression of virus-encoded late genes, which are critical for viral assembly and whose transcription initiates only after the onset of viral DNA replication. The vTAs in Kaposi's sarcoma-associated herpesvirus (KSHV) are ORF18, ORF24, ORF30, ORF31, ORF34, and ORF66. While the general organization of the vTA complex has been mapped, the individual roles of these proteins and how they coordinate to activate late gene promoters remain largely unknown. Here, we performed a comprehensive mutational analysis of the conserved residues in ORF18, which is a highly interconnected vTA component. Surprisingly, the mutants were largely selective for disrupting the interaction with ORF30 but not the other three ORF18 binding partners. Furthermore, disrupting the ORF18-ORF30 interaction weakened the vTA complex as a whole, and an ORF18 point mutant that failed to bind ORF30 was unable to complement an ORF18 null virus. Thus, contacts between individual vTAs are critical as even small disruptions in this complex result in profound defects in KSHV late gene expression.

IMPORTANCE Kaposi's sarcoma-associated herpesvirus (KSHV) is the etiologic agent of Kaposi's sarcoma and other B-cell cancers and remains a leading cause of death in immunocompromised individuals. A key step in the production of infectious virions is the transcription of viral late genes, which generates capsid and structural proteins and requires the coordination of six viral proteins that form a complex. The role of these proteins during transcription complex formation and the importance of protein-protein interactions are not well understood. Here, we focused on a central component of the complex, ORF18, and revealed that disruption of its interaction with even a single component of the complex (ORF30) prevents late gene expression and completion of the viral lifecycle. These findings underscore how individual interactions between the late gene transcription components are critical for both the stability and function of the complex.

KEYWORDS KSHV, Kaposi's sarcoma-associated herpesvirus, ORF18, ORF30, herpesvirus, late gene transcription

A broadly conserved feature of the life cycle of double-stranded DNA (dsDNA) viruses is that replication of the viral genome licenses transcription of a specific class of viral transcripts termed late genes. There is an intuitive logic behind this coupling as late genes encode proteins that participate in progeny virion assembly and egress and, thus, are not needed until newly synthesized genomes are ready for packaging. Additionally, late gene transcription requires ongoing DNA replication, and in the gammaherpesviruses Kaposi's sarcoma-associated herpesvirus (KSHV) and Epstein-Barr virus (EBV), the increase in template abundance appears insufficient to

Citation Castañeda AF, Glaunsinger BA. 2019. The interaction between ORF18 and ORF30 is required for late gene expression in Kaposi's sarcoma-associated herpesvirus. J Virol 93:e01488-18. https://doi.org/10.1128/JVI.01488-18.

Editor Rozanne M. Sandri-Goldin, University of California, Irvine

Address correspondence to Britt A. Glaunsinger, glaunsinger@berkeley.edu.

Received 27 August 2018
Accepted 5 October 2018
Accepted manuscript posted online 10 October 2018
Published 10 December 2018

explain the robust transcription of late genes whose products are required in large amounts (1).

While the mechanisms underlying late gene activation can vary across viral families, in the beta- and gammaherpesviruses, late gene promoters are strikingly minimalistic and primarily consist of a modified TATA box (TATT) and ~10 to 15 bp of variable flanking sequence (2–5). Despite this sequence simplicity, their transcription requires a dedicated set of at least six conserved viral transcriptional activators (vTAs) whose precise roles are only beginning to be uncovered. In KSHV, the vTAs are encoded by open reading frames (ORFs) 18, 24, 30, 31, 34, and 66 (6–15). The best-characterized of the vTAs is a viral TATA-binding protein (TBP) mimic, encoded by ORF24 in KSHV, which binds both the late gene promoter and RNA polymerase II (Pol II) (4, 8, 16, 17). Beyond the viral TBP mimic, the only other vTA with a documented transcription-related function is pUL79 (homologous to KSHV ORF18) in human cytomegalovirus (HCMV), which promotes transcription elongation at late times of infection (18). Roles for the remaining vTAs remain largely elusive although the KSHV ORF34 protein and its murine cytomegalovirus (MCMV) homolog pM95 may function as hub proteins as they interact with numerous other vTAs (7, 9, 19). In addition to the six conserved vTAs, in EBV the kinase activity of BGLF4 (homologous to KSHV ORF36) also contributes to the expression of late genes (20, 21).

Studies in both beta- and gammaherpesviruses indicate that the vTAs form a complex, the general organization of which has been mapped in MCMV and KSHV (7, 9, 10, 19) (Fig. 1A). Notably, several recent reports demonstrate that specific interactions between the vTAs are critical for late gene transcription. In MCMV, mutation of conserved residues in pM91 (homologous to KSHV ORF30) that disrupt its interaction with pM79 (homologous to KSHV ORF18) renders the virus unable to transcribe late genes (19). Similarly, the interaction between KSHV ORFs 24 and 34 can be abrogated by a single amino acid mutation in ORF24 which prevents late gene transcription (9). Further delineating these contacts should provide foundational information relevant to understanding vTA complex function.

The precise role of KSHV ORF18 in late gene transcription remains unknown; however, it is predicted to interact with four of the five other vTAs (ORFs 30, 31, 34, and 66), suggesting that, like ORF34, it may play a central role in vTA complex organization (7, 9). Here, we performed an interaction screen of mutants of ORF18 to comprehensively evaluate the roles of its conserved residues in mediating pairwise vTA binding. We reveal that ORF30 is particularly sensitive to mutation in ORF18, enabling isolation of mutants that selectively abrogate this interaction while retaining the contacts between ORF18 and the other vTAs. Disrupting the ORF18-ORF30 interaction not only prevents KSHV late gene transcription as measured by K8.1 expression but also appears to weaken assembly of the remaining vTA complex. These findings underscore the key role that ORF18 plays in late gene transcription and suggest that disrupting just one of its interactions has a destabilizing effect on the vTA complex as a whole.

(This article was submitted to an online preprint archive [22]).

RESULTS

ORF18 interacts with ORF30, ORF31, ORF34, and ORF66. Previous work using a split luciferase-based interaction screen suggested that ORF18 is highly interconnected with other viral late gene activators as it interacted with the majority of the proteins in the viral transcription preinitiation complex (vPIC) (9). To independently confirm the binding of ORF18 to ORFs 30, 31, 34, and 66 in the absence of other viral factors, we assessed its ability to coimmunoprecipitate (co-IP) with each of these vTAs in transfected HEK293T cells. Consistent with the screening data, ORF18 carrying three copies of a FLAG tag (ORF18-3×FLAG) interacted robustly with C-terminal 2×Strep-tagged versions of ORF30, ORF31, and ORF66 (Fig. 1B to D). Although ORF18-3×FLAG did not interact with ORF34 tagged on its C terminus, the interaction was recovered upon moving the 2×Strep tag to the N terminus of ORF34 (Fig. 1E). Furthermore, we consistently observed that the expression of ORF30 was higher when it was coex-

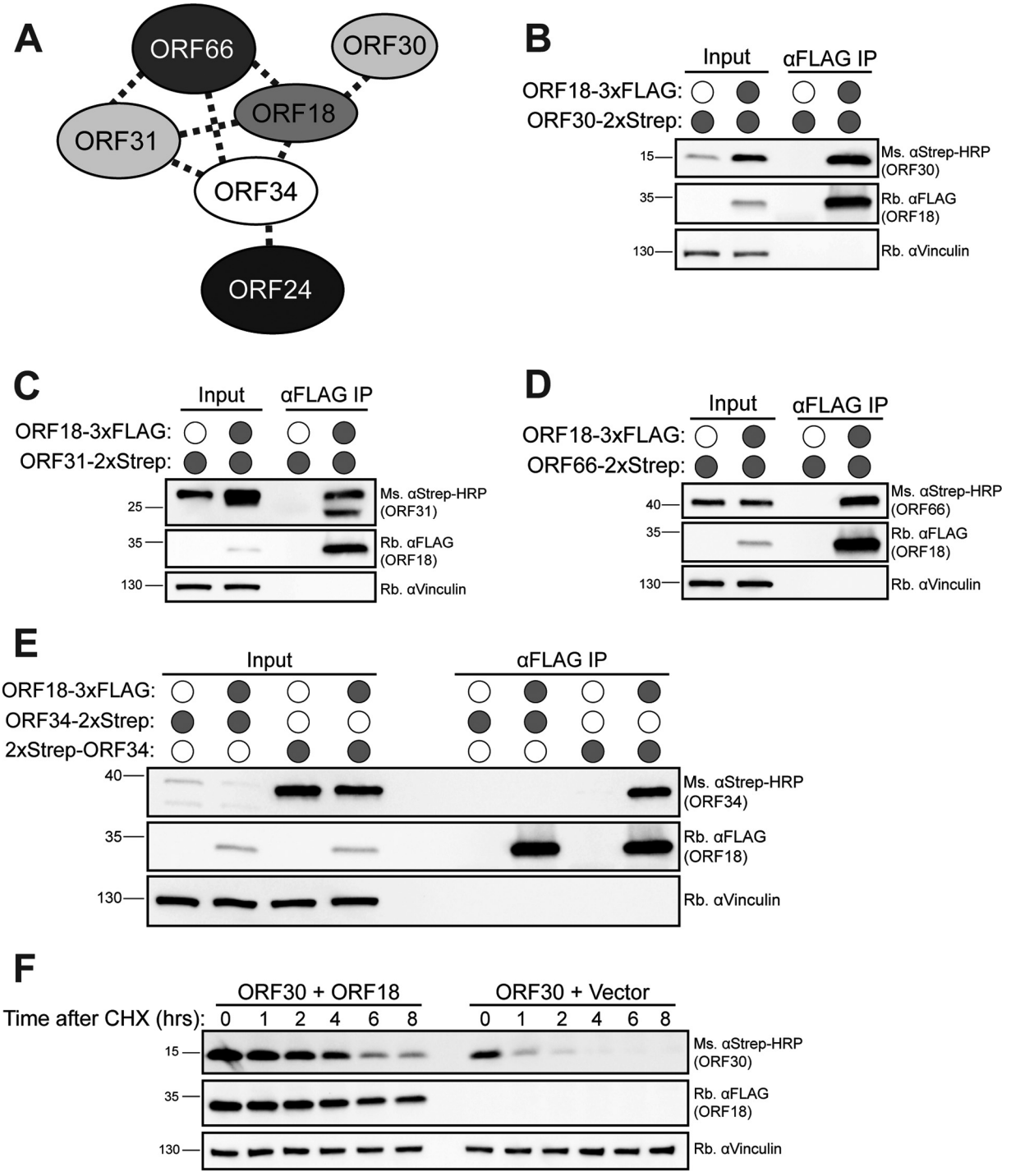

FIG 1 ORF18 interacts with ORFs 30, 31, 34, and 66. (A) Diagram of vTA interactions in KSHV. (Republished from reference 9.) (B to E) HEK293T cells were transfected with the indicated vTA plasmids and then subjected to co-IP using anti-FLAG beads followed by Western blot analysis with the indicated antibody to detect ORF18 and either ORF30 (B), ORF31 (C), ORF66 (D), or ORF34 (E). Input represents 2.5% of the lysate used for co-IP. Vinculin served as a loading control. (F) HEK293T cells were transfected with the indicated vTA plasmids. At 24 h posttransfection, cycloheximide (CHX) was added to a final concentration of 100 μg/ml, and samples were collected at the indicated time points after the addition of cycloheximide. Whole-cell lysate (25 μg) was resolved using SDS-PAGE, followed by Western blotting with the indicated antibodies. Vinculin served as a loading control. Rb, rabbit; Ms, mouse.

pressed with ORF18 than when it was transfected with a vector control, suggesting that ORF18 may stabilize ORF30 (Fig. 1B). To determine whether ORF18 had a stabilizing effect on ORF30, the half-life of ORF30 was measured in both the presence and absence of ORF18. As can be seen in Fig. 1F, stability of ORF30 increased significantly when it was coexpressed with ORF18.

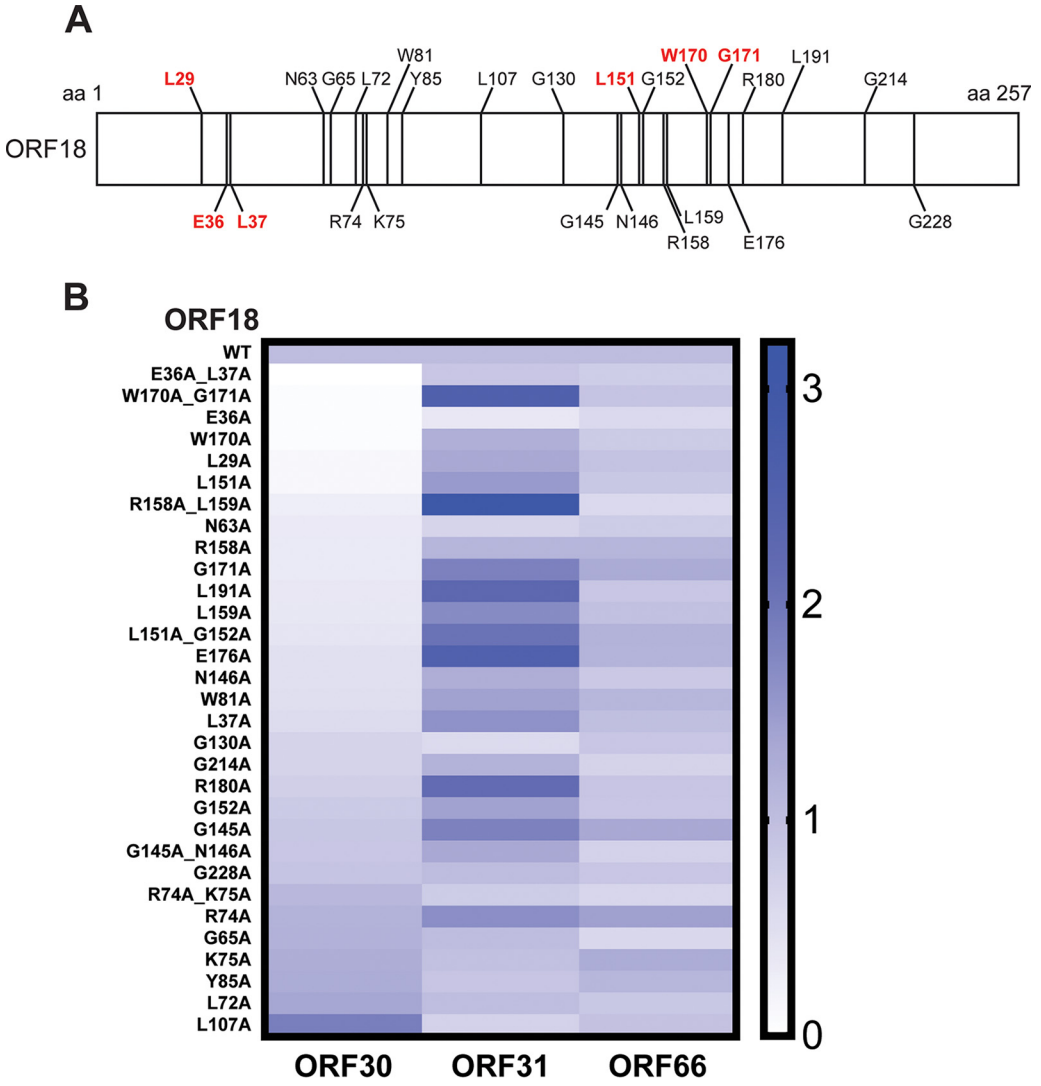

FIG 2 ORF18 mutant screen for interactions with ORFs 30, 31, and 66. (A) Diagram depicting the conserved residues in KSHV ORF18 in a MUSCLE alignment with MHV68 ORF18, EBV BVLF1, HCMV pUL79, MCMV pM79, and BHV4 ORF18. Red denotes amino acids (aa) found to have interactions at <10% of the WT level with any of the vTAs. (B) Heat map of the co-IP efficiency of each ORF18 mutant against ORFs 30, 31, and 66.

An interaction screen of ORF18 mutants reveals the role of conserved residues in interactions with the other vTAs. To evaluate the importance of the interaction between ORF18 and its individual vTA contacts, we aimed to identify point mutations that disrupted binding to individual vTAs but did not destroy the integrity of the complex. Since the late gene vTA complex is conserved across the beta- and gammaherpesviruses, we reasoned that the individual points of contact might depend on conserved amino acid residues. We performed a multiple sequence alignment between KSHV ORF18 and its homologs in five other beta- and gammaherpesviruses (MHV68 ORF18, HCMV pUL79, MCMV pM79, EBV BVLF1, and bovine herpesvirus [BHV] ORF18) using MUSCLE (23). The sequence alignment revealed 25 single conserved residues, including six pairs of adjacent conserved residues, which are depicted in Fig. 2A, which shows a schematic of the primary structure of ORF18 and the positions of conserved residues. We mutated each of the 25 conserved residues to alanines in ORF18-3×FLAG and made double alanine mutations in the six cases of adjacent conserved residues (Fig. 2A). Each of these 31 mutants was screened individually for the ability to interact with ORFs 30, 31, and 66 by co-IP followed by Western blotting (data not shown). To

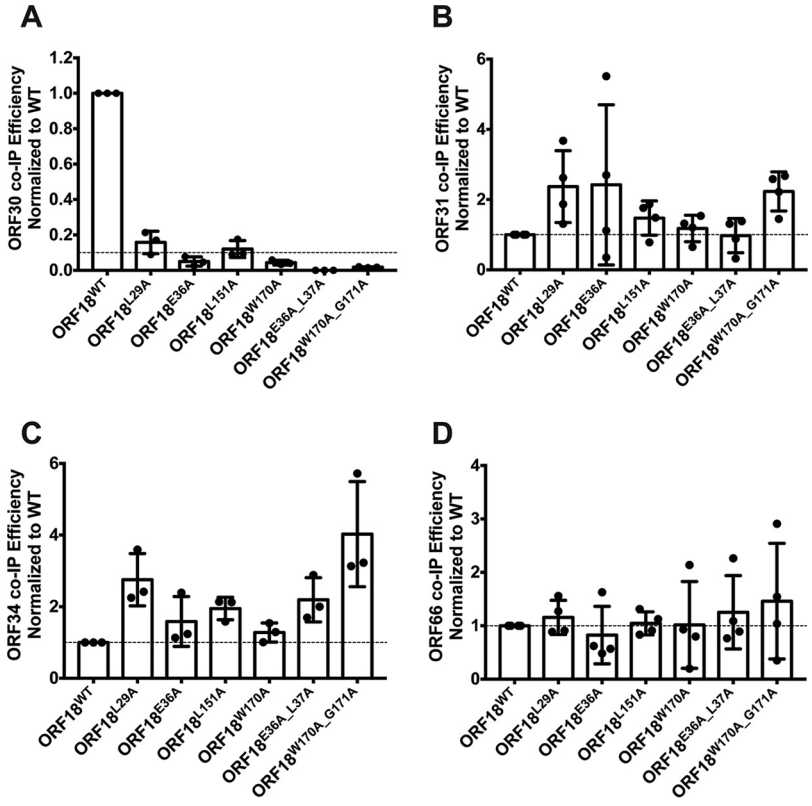

FIG 3 Six ORF18 mutants are consistently defective for interaction with ORF30. (A to D) HEK293T cells were transfected with the indicated vTA plasmids and then subjected to co-IP using anti-FLAG beads, followed by Western blot analysis to detect the ability of the WT or mutant ORF18 to interact with ORF30 (A), ORF31 (B), ORF34 (C), and ORF66 (D). The co-IP efficiencies were calculated as described in the text for 3 to 4 independent experimental replicates and plotted as bar graphs. In panel A, the dotted line represents $y = 0.1$, and in panels B to D, the dotted line represents $y = 1.0$.

account for differences in expression levels between the ORF18 mutants, we calculated the co-IP efficiency of each of the mutants, as described in Materials and Methods. These data were used to generate a heat map, which displays the pairwise interaction efficiencies on a color scale where lighter blocks represent reduced binding and darker blocks represent increased binding relative to binding of the wild type (WT) ORF (Fig. 2B). Overall, the data revealed that ORF30 was the most sensitive to mutations in ORF18, as 24 out of the 31 mutants displayed reduced or no binding. ORF31 showed variable sensitivity to ORF18 mutation (with some mutants even increasing the interaction efficiency), while the ORF66-ORF18 interaction was relatively refractory to the ORF18 point mutations (Fig. 2B).

We focused on the six ORF18 mutants that exhibited <10% co-IP efficiency, relative to the WT level, with any vTA in our initial screen (L29A, E36A, L151A, W170A, and double mutants E36A_L37A and W170A_G171A) (highlighted in red in Fig. 2A). These were rescreened three to four times independently in co-IP assays with vTA component ORFs 30, 31, 34, and 66, and the co-IP efficiencies were calculated as described in Materials and Methods and then plotted relative to values obtained for WT ORF18 (Fig. 3A to D). All six of these ORF18 mutants had severe defects in their abilities to co-IP ORF30, but none were consistently different from the WT ORF18 for interaction with ORFs 31, 34, and 66 (Fig. 3B to D). Among the six mutants, ORF18^{E36A_L37A} and ORF18^{W170A_G171A} showed no detectable binding to ORF30, with ORF18^{E36A_L37A} retaining nearly WT levels of interaction with the remaining vTAs.

ORF18 point mutants that weaken the interaction between ORF18 and ORF30 have a reduced capacity to activate the K8.1 late gene promoter. A reporter assay has been developed in which the coexpression of the six individual vTAs can specifically

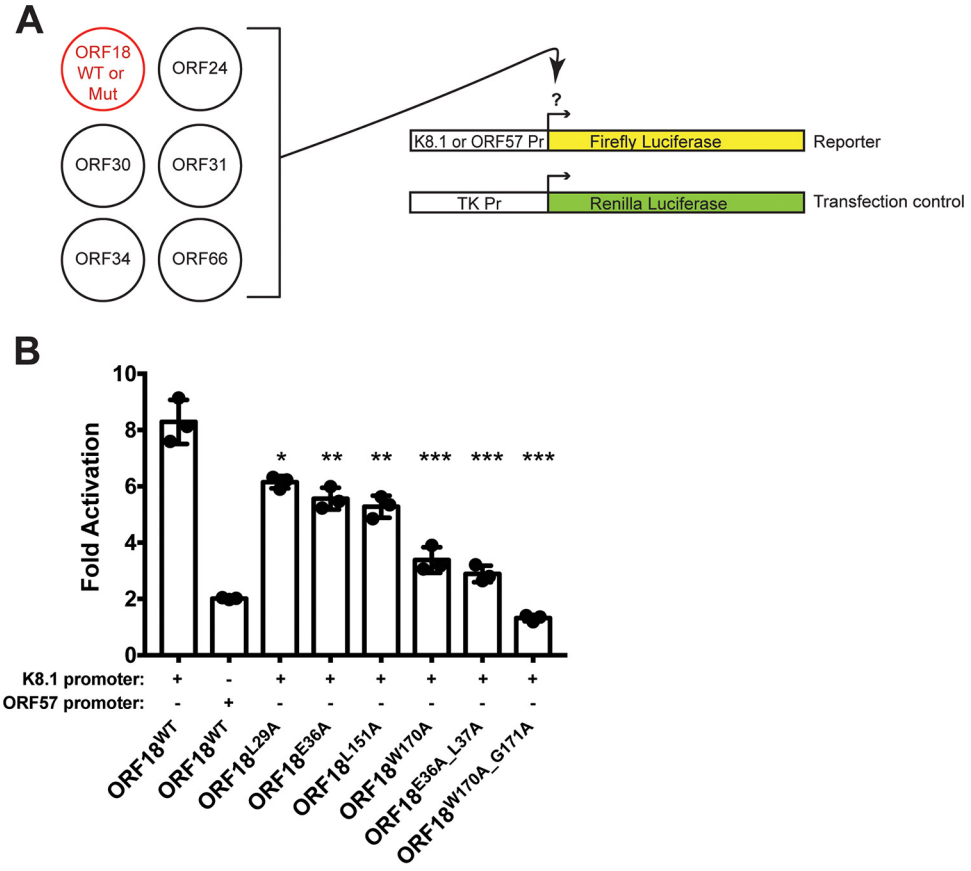

FIG 4 Impairing the interaction between ORF18 and ORF30 reduces activation of the late K8.1 promoter. (A) Diagram depicting the vector combinations that were transfected for the late gene reporter assay. TK, thymidine kinase; Pr, promoter. (B) HEK293T cells were transfected with the vTA plasmids, including the WT or mutant (Mut) ORF18, the K8.1 or ORF57 promoter reporter plasmid, and the pRL-TK *Renilla* plasmid as a transfection control. At 24 h posttransfection the lysates were harvested, and luciferase activity was measured. Data shown are from 3 independent biological replicates, with statistics calculated using an unpaired *t* test (*, $P < 0.05$; **, $P < 0.005$; ***, $P < 0.0007$).

activate a KSHV (or EBV) late gene promoter in transfected HEK293T cells (9, 10). We used this assay as an initial proxy for the ability of the six ORF18 mutants described above to activate late gene transcription. HEK293T cells were cotransfected with each of the vTAs, including either the WT or mutant ORF18, and firefly luciferase reporter plasmids driven by either the late K8.1 promoter or, as a control, the early ORF57 promoter (Fig. 4A). A plasmid containing constitutively expressed *Renilla* luciferase was cotransfected with each sample to normalize for transfection efficiency. As expected, inclusion of WT ORF18 with the remaining vTA complex resulted in specific activation of the K8.1 late promoter but not of the early ORF57 promoter (Fig. 4B). ORF18 mutants L29A, E36A, and L151A modestly reduced activation of the late promoter, whereas more significant defects were observed with mutants W170A, E36A_L37A, and W170A_G171A (Fig. 4B). Although ORF18^{W170A_G171A} had the most pronounced transcriptional defect, this mutant showed somewhat more variability than ORF18^{E36A_L37A} in its interactions with the other vTA components (Fig. 3 and 4). Thus, we considered ORF18^{E36A_L37A} to be the top candidate for selectively analyzing the importance of the ORF18-ORF30 interaction for KSHV late gene transcription.

The interaction between ORF18 and ORF30 affects assembly of the vTA complex. The transcriptional defect of the ORF18^{E36A_L37A} mutant in the reporter assay could be due to a defect in assembly of the complex or due to defects in downstream events. To distinguish between these possibilities, WT or mutant ORF18-3×FLAG was cotransfected into HEK293T cells with each of the other Strep-tagged vTAs. We then

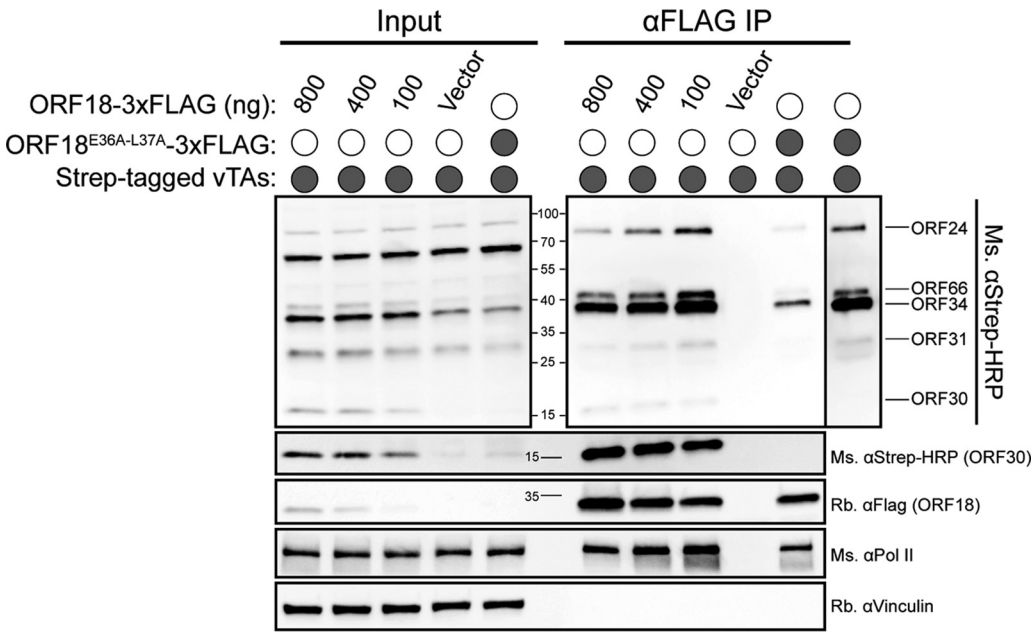

FIG 5 Disrupting the interaction between ORF18 and ORF30 weakens the assembly of the vTA complex. HEK293T cells were transfected with the indicated vTA plasmids and then subjected to co-IP using anti-FLAG beads, followed by Western blot analysis with the indicated antibody. The boxed lane on the far right represents a longer exposure of the ORF18^{E36A_L37A} IP. Input represents 2.5% of the lysate used for co-IP. Vinculin was used as a loading control.

performed an anti-FLAG IP, revealing that purification of WT ORF18 led to co-IP of the complete vTA complex including Pol II, which has been shown to interact with ORF24 in KSHV (8) (Fig. 5). We noted that in this assay ORF18^{E36A_L37A} was more weakly expressed than WT ORF18, so to compare complex formation with equivalent amounts of each protein, we titrated down the amount of WT ORF18 to match the levels of ORF18^{E36A_L37A}. Similar to our observation in a pairwise co-IP (Fig. 1B), the ORF30 protein abundance decreased as the expression of ORF18 was reduced (Fig. 5); however, the complete vTA complex still copurified even with reduced levels of WT ORF18 (Fig. 5). Notably, the vTA complex was recovered at lower levels in the presence of ORF18^{E36A_L37A}. When imaged at a longer exposure, all of the vTAs, with the exception of ORF30, remained associated with ORF18^{E36A_L37A} (Fig. 5, far right panel). Thus, the selective loss of the ORF18-ORF30 interaction may reduce the overall stability of the vTA complex.

The interaction between ORF18 and ORF30 is crucial for expression of the late gene K8.1. Next, to characterize the effect of ORF18^{E36A_L37A} on the viral replication cycle, we tested the ability of this mutant to complement the late gene expression defect of a KSHV mutant lacking ORF18 (18.stop) (6). The renal carcinoma cell line iSLK harbors the virus (either WT or 18.stop) in a latent state, which can be reactivated upon expression of the doxycycline-inducible major lytic transactivator RTA and treatment with sodium butyrate. Using lentiviral transduction, we generated stable, doxycycline-inducible versions of the 18.stop iSLK cells expressing either ORF18-3×FLAG or ORF18^{E36A_L37A}-3×FLAG (18.stop.ORF18^{WT} or 18.stop.ORF18^{E36A_L37A}, respectively). The cells were assayed 72 h after lytic reactivation for their ability to replicate DNA, express early and late proteins, and produce progeny virions. Although we observed a modest decrease of viral DNA replication in the 18.stop cells, as measured by quantitative PCR (qPCR), upon complementation with either WT ORF18 or ORF18^{E36A_L37A}, the levels of DNA replication were not significantly different from those in iSLK cells infected with WT KSHV (Fig. 6A). Notably, the 18.stop.ORF18^{E36A_L37A} cell line expressed more ORF18 than the 18.stop.ORF18^{WT} cell line, in contrast to the reduced expression of the mutant in HEK293T cells (Fig. 6B, compare to levels in Fig. 5). However, while both reactivated 18.stop.ORF18^{WT} and 18.stop.ORF18^{E36A_L37A} cell lines expressed

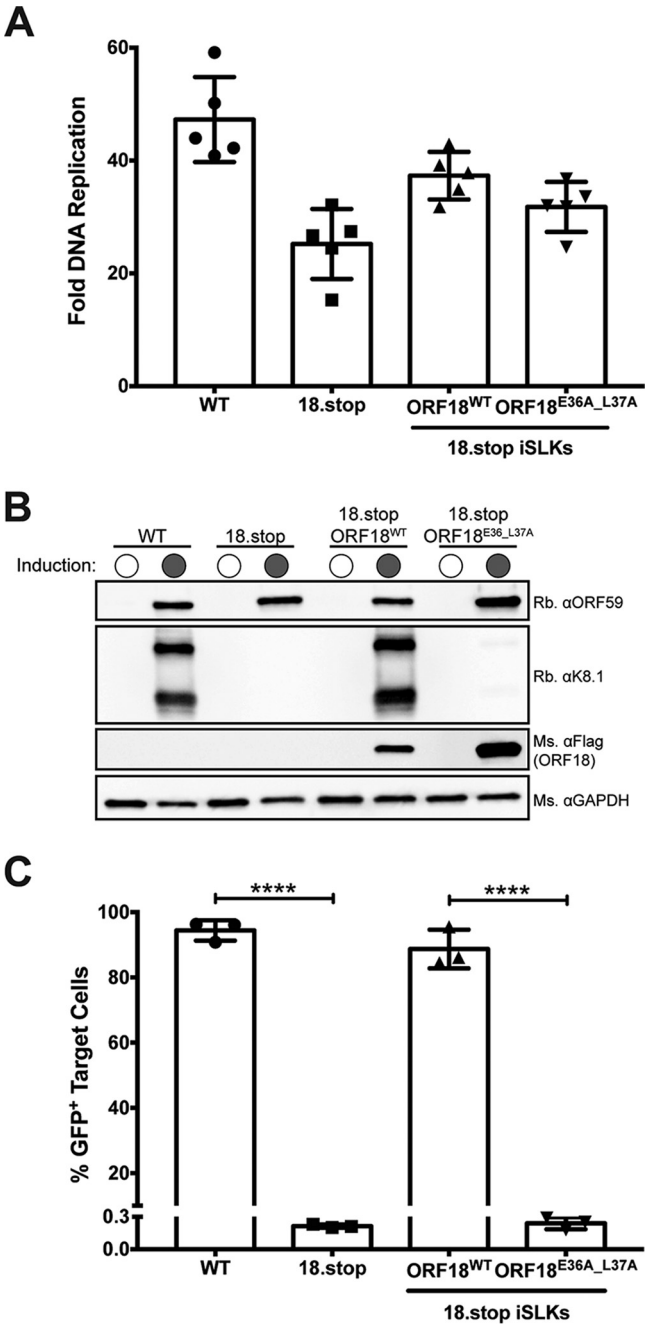

FIG 6 Characterizing the effect of the E36A_L37A ORF18 mutation on the virus. (A) iSLK cells latently infected with WT KSHV, 18.Stop KSHV, or 18.Stop complemented with ORF18^{WT} or ORF18^{E36A_L37A} were induced to enter the lytic cycle with 1 μg/ml doxycycline and 1 mM sodium butyrate. At 72 h postinduction, DNA was isolated, and viral DNA fold replication was measured by qPCR before and after induction of the lytic cycle. Data shown are from 5 independent biological replicates. (B) Western blots of the expression of the early protein ORF59, the late protein K8.1, ORF18^{WT}, and ORF18^{E36A_L37A} in the indicated cell lines induced as described for panel A. GAPDH was used as a loading control. (C) HEK293T target cells were spinfected with filtered supernatant from induced cells. Progeny virion production was measured 24 h after supernatant transfer by flow cytometry of GFP-positive (GFP$^+$) target cells. Data shown are from 3 independent biological replicates with statistics calculated using an unpaired *t* test (****, $P < 0.0001$).

equivalent levels of the ORF59 early protein, only 18.stop.ORF18^{WT} was able to rescue expression of the model late gene K8.1 (Fig. 6B).

We then evaluated the level of KSHV virion production from the parental WT KSHV-infected iSLK cells, as well as from the 18.stop, 18.stop.ORF18^{WT}, and

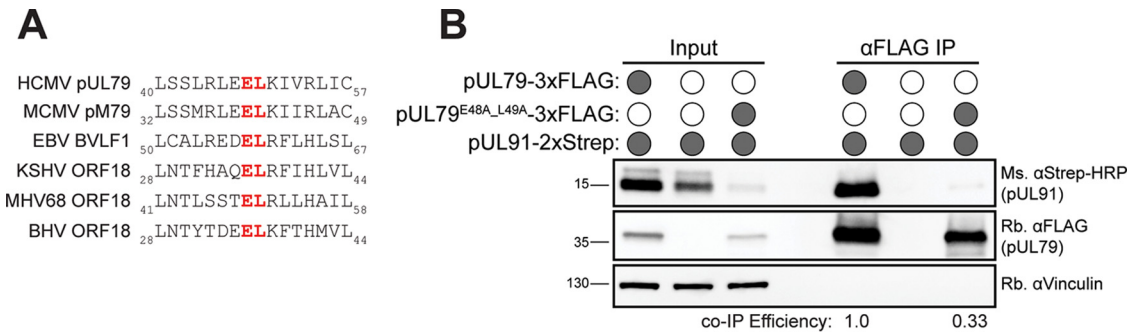

FIG 7 Mutating E48_L49 in pUL79 disrupts its interaction with pUL91. (A) MUSCLE multiple sequence alignment for HCMV pUL79 and homologs showing the location of conserved amino acids (in red) that correspond to E36_L37 in KSHV ORF18. (B) HEK293T cells were transfected with the indicated plasmids and then subjected to co-IP using anti-FLAG beads, followed by Western blot analysis with the indicated antibody. To normalize for the difference in expression levels of pUL91 under the different transfection conditions, the co-IP efficiency was multiplied by the fold expression of pUL91 in the presence of WT pUL79 versus that with E48A_L49A pUL79. Input represents 2.5% of lysate used for co-IP. Vinculin was used as a loading control.

18.stop.ORF18^{E36A_L37A} cell lines, using a supernatant transfer assay. KSHV produced from iSLK cells contains a constitutively expressed green fluorescent protein (GFP), enabling quantitation of infected recipient cells by flow cytometry (24). Consistent with a late gene expression defect, neither the 18.stop nor the 18.stop.ORF18^{E36A_L37A} cell line was able to produce progeny virions, whereas virion production in the 18.stop.ORF18^{WT} cells was indistinguishable from that in the WT KSHV-infected iSLK cells (Fig. 6C). Collectively, these data demonstrate that the specific interaction between ORF18 and ORF30 is essential for K8.1 late gene expression and virion production during KSHV infection.

The analogous mutation in HCMV pUL79 disrupts its interaction with pUL91. As shown in Fig. 7A, the E36_L37 residues are conserved across the beta- and gammaherpesvirus ORF18 homologs. To determine whether these amino acids are similarly important in a betaherpesvirus, we engineered the corresponding double mutation in HCMV pUL79 (pUL79^{E48A_L49A}-3×FLAG). Similar to our observation with KSHV ORF30, HCMV pUL91 protein expression was significantly decreased in the absence of its WT pUL79 binding partner (Fig. 7B). This is consistent with the idea that pUL79 binding stabilizes pUL91. Furthermore, in co-IP assays we detected a robust interaction between pUL79 and pUL91, which was impaired in the presence of pUL79^{E48A_L49A}, even when we accounted for the expression level differences of pUL91 (Fig. 7B). This suggests that the overall protein-protein interface may be conserved in the analogous ORF18-ORF30 interaction across the beta- and gammaherpesviruses.

DISCUSSION

Elucidating the architecture of the six-member vPIC complex is central to understanding the mechanism underlying viral late gene expression in beta- and gammaherpesviruses. Although their functions are largely unknown, each of these viral transcription regulators is essential for late gene promoter activation, and evidence increasingly suggests that their ability to form a complex is crucial for transcriptional activity (9, 10, 19). Here, we reveal that selective disruption of an individual protein-protein contact between KSHV ORF18 and ORF30 within the vPIC is sufficient to abrogate K8.1 late gene expression and virion production in infected cells, emphasizing the sensitivity of the complex to organizational perturbation.

We selected ORF18 for mutational screening due to its ability to form pairwise interactions with the majority of other vPIC components, which suggested that it might serve as an organizational hub for vPIC assembly, similar to what has been proposed for ORF34 (7, 9). However, the 31 tested mutants of ORF18 revealed that conserved residues across the length of the protein are extensively—and largely selectively—required for ORF30 binding. This is in contrast to the interaction between the vPIC components ORF24 and ORF34, where the interaction can be localized to a 17-amino-

acid stretch of ORF24 (9). The observation that the majority of the point mutations in ORF18 that disrupt the interaction with ORF30 do not affect its binding to ORFs 31, 34, and 66 indicates that these mutations do not significantly alter the overall folding or structure of ORF18. In MCMV, the organization of the vTA complex is similar to that of KSHV, except that pM92 (homologous to KSHV ORF31) interacts with pM87 (homologous to KSHV ORF24), whereas in KSHV this interaction is bridged through ORF34 (19). Our data complement recent findings in MCMV, in which mutations of the ORF30 homolog (pM91) that perturb the interaction with the ORF18 homolog (pM79) similarly cause a defect in the expression of late genes (19). Thus, mutations that disrupt the ORF18-ORF30 protein-protein interface in either protein cause the same phenotype.

The ORF18-ORF30 interaction appears sensitive to single amino acid changes in the protein-protein interface. The ORF18^{E36A_L37A} mutation does not impair binding to its other vPIC partners in pairwise co-IP experiments, and ORF30 does not engage in pairwise interactions with vPIC components other than ORF18 (7, 9). It is therefore notable that the efficiency of the vPIC complex assembly is reduced in HEK293T cells in the presence of the ORF18^{E36A_L37A} mutant, suggesting that the ORF18-ORF30 interaction contributes to the stability of the complex as a whole. The interaction between ORF18 and ORF30 may change the conformation of ORF18, allowing it to interact more strongly with the other vTAs. Alternatively, the E36A_L37A mutation may contribute to binding defects between ORF18 and the other vTAs that are not observed with pairwise interactions but are enhanced in the presence of all the ORF18 binding partners.

We observed that ORF30 protein expression was consistently higher in the presence of WT ORF18 or ORF18 mutants that retained ORF30 binding, suggesting that ORF18 helps stabilize ORF30. *In silico* protein stability prediction studies have suggested that protein stability is in part affected by protein length, where proteins that are less than 100 amino acids tend to be less stable (25, 26). One explanation for the higher expression of ORF30 in the presence of ORF18 could therefore be that the 77-amino-acid ORF30 is protected from degradation by ORF18. Another possibility is that ORF18 helps keep ORF30 correctly folded; this has been proposed as a mechanism that stabilizes proteins which have interaction partners (27). The interaction-induced stability of a protein often correlates with the relative concentration of its binding partners (27), as we observed when we titrated down the amount of ORF18 in the context of the complete vTA complex. A similar observation has been made between KSHV proteins ORF36 and ORF45, where ORF36 was dependent on the interaction with ORF45 for stabilization (28). We did not observe a similar correlation with levels of the other ORF18-associated vPIC proteins, and, thus, their stability may not require protective interactions. We also observed a stabilizing effect of pUL79 on pUL91, indicating this may be a conserved feature of this interaction in other beta- and gammaherpesviruses.

The fact that the late gene expression defect of the ORF18^{E36A_L37A} mutant is exacerbated in the context of the virus, compared to that in the plasmid promoter activation assay, likely reflects the fact that the plasmid assay measures basal promoter activation but misses other regulatory components of this cascade. For example, the origin of lytic replication is required in *cis* for late gene expression in related gammaherpesviruses (3, 29), and the reporter assay does not capture the important contribution of viral DNA replication toward late gene expression. This may explain why some mutants that are defective for ORF30 binding (e.g., L29A, E36A, and L151A) retain partial plasmid promoter activity; perhaps some weak binding between ORF18 and ORF30 enables basal activation of the promoter in a context where the vPIC components are overexpressed. Alternatively, some of the mutations may cause ORF18 to bind to ORF30 more transiently, but their vPIC interaction becomes stabilized in the presence of a late gene promoter.

In summary, the absence of K8.1 late gene expression in the KSHV ORF18.stop-infected cells complemented with ORF18^{E36A_L37A} may derive from a cascade of phenotypes: the failure to recruit ORF30 to the vPIC, the ensuing reduction in the efficiency of overall vPIC complex assembly, and the reduced stability of ORF30 (if it also has additional vPIC-independent functions). Ultimately, generating antibodies that

recognize the endogenous KSHV vPIC components will enable these phenotypes to be explored further during infection. In addition, information about the three-dimensional structure of the vPIC would significantly enhance our understanding of this unique transcription complex as it is becoming increasingly clear that even small disruptions to the complex dramatically impact completion of the viral life cycle.

MATERIALS AND METHODS

Plasmids and plasmid construction. To generate ORF18-3×FLAG pCDNA4, ORF18 was subcloned into the BamHI and NotI sites of pCDNA-3×FLAG. The point mutations in ORF18 were generated using two-primer site-directed mutagenesis with Kapa HiFi polymerase (Roche) with primers 1 to 62 listed in Table 1. All subsequent plasmids described below were generated using InFusion cloning (Clontech) unless indicated otherwise. To generate plasmid pLVX-TetOneZeo, Zeocin resistance was PCR amplified out of plasmid pLJM1-EGFP-Zeo with primers 63/64 (Table 1) and used to replace the puromycin resistance in pLVX-TetOne-Puro (Clontech) using the AvrII and MluI restriction sites. To generate pLVX-TetOneZeo-ORF18^{WT}-3×FLAG and pLVX-TetOneZeo-ORF18^{E36A_L37A}-3×FLAG, ORF18^{WT}-3×FLAG and ORF18^{E36_37A}-3×FLAG were PCR amplified from each respective pCDNA4 plasmid using primers 71/72 and inserted into the EcoRI and BamHI sites of pLVX-TetOne-Zeo. To generate UL79-3×FLAG pCDNA4 and UL91-2×Strep pCDNA4, UL79 was PCR amplified with primers 67/68 (Table 1), and UL91 was PCR amplified with primers 69/70 (Table 1) from the HCMV Towne strain, which was kindly provided by Laurent Coscoy, and cloned into the BamHI and NotI sites of 3×FLAG (Cterm) pCDNA4 (where Cterm indicates a C-terminal tag) or 2×Strep (Cterm) pCDNA4. UL79^{E48A_L49A} was generated with two-primer site-directed mutagenesis using Kapa HiFi polymerase with primers 73/74 (Table 1). To make 2×Strep-ORF34 pCDNA4, ORF34 was PCR amplified from ORF34-2×Strep pCDNA4 with primers 65/66 and cloned into the NotI and XbaI sites of 2×Strep (Nterm) pCDNA4 (where Nterm indicates an N-terminal tag). Plasmid K8.1 Pr pGL4.16 contains the minimal K8.1 promoter, and ORF57 Pr pGL4.16 contains a minimal ORF57 early gene promoter; both have been described previously (9). Plasmids ORF18-2×Strep pCDNA4, ORF24-2×Strep pCDNA4, ORF30-2×Strep pCDNA4, ORF31-2×Strep pCDNA4, ORF34-2×Strep pCDNA4, and ORF66-2×Strep pCDNA4 have been previously described (8). Plasmid pRL-TK (Promega) was kindly provided by Russel Vance. Lentiviral packaging plasmids psPAX2 (plasmid number 12260; Addgene) and pMD2.G (plasmid number 12259; Addgene) were gifts from Didier Trono.

Cells and transfections. HEK293T cells (ATCC CRL-3216) were maintained in Dulbecco's modified Eagle's medium (DMEM) supplemented with 10% fetal bovine serum (FBS) (Seradygm). The iSLK renal carcinoma cell line harboring the KSHV genome on the bacterial artificial chromosome BAC16 and a doxycycline-inducible copy of the KSHV lytic transactivator RTA (iSLK-BAC16) have been described previously (24). iSLK-BAC16-ORF18.stop cells that contain a stop mutation in ORF18 were kindly provided by Ting-Ting Wu (6). iSLK-BAC16 and iSLK-BAC16-ORF18.stop were maintained in DMEM supplemented with 10% FBS, 1 mg/ml hygromycin, and 1 μg/ml puromycin (iSLK-BAC16 medium). iSLK-BAC16-ORF18.stop cells were complemented by lentiviral transduction with ORF18^{WT}-3×FLAG or ORF18^{E36A_L37A}-3×FLAG. To generate the lentivirus, HEK293T cells were cotransfected with pLVX-TetOneZeo-ORF18^{WT}-3×FLAG or pLVX-TetOneZeo-ORF18^{E36A_L37A}-3×FLAG along with the packaging plasmids pMD2.G and psPAX2. After 48 h, the supernatant was harvested and syringe filtered through a 0.45-μm-pore-size filter (Millipore). The supernatant was diluted 1:2 with DMEM, and Polybrene was added to a final concentration of 8 μg/ml. A total of 1×10^6 iSLK-BAC16-ORF18.stop freshly trypsinized cells were spinfected in a six-well plate for 2 h at 500 × *g*. After 24 h the cells were expanded to a 10-cm tissue culture plate and selected for 2 weeks in iSLK-BAC16 medium supplemented with 325 μg/ml Zeocin (Sigma). For DNA transfections, HEK293T cells were plated and transfected after 24 h at 70% confluence with PolyJet (SignaGen).

Immunoprecipitation and Western blotting. Cell lysates were prepared 24 h after transfection by washing and pelleting cells in cold phosphate-buffered saline (PBS), resuspending the pellets in IP lysis buffer (50 mM Tris-HCl, pH 7.4, 150 mM NaCl, 1 mM EDTA, 0.5% NP-40, and protease inhibitor [Roche]), and rotating the samples for 30 min at 4°C. Lysates were cleared by centrifugation at 21,000 × *g* for 10 min, and then 1 mg (for pairwise interaction IPs) or 2 mg (for the entire late gene complex IPs) of lysate was incubated with prewashed M2 anti-FLAG magnetic beads (Sigma) overnight. The beads were washed three times for 5 min each with IP wash buffer (50 mM Tris-HCl pH 7.4, 150 mM NaCl, 1 mM EDTA, 0.05% NP-40) and eluted with 2× Laemmli sample buffer (Bio-Rad).

Lysates and elutions were resolved by SDS-PAGE and subjected to Western blotting in TBST (Tris-buffered saline, 0.2% Tween 20) using the following primary antibodies: Strep-horseradish peroxidase (HRP) (1:2500; Millipore), rabbit anti-FLAG (1:3,000; Sigma), mouse anti-FLAG (1:1,000; Sigma), rabbit anti-vinculin (1:1,000; Abcam), mouse anti- glyceraldehyde-3-phosphate dehydrogenase (GAPDH) (1:1,000; Abcam), mouse anti-Pol II C-terminal domain (CTD) clone 8WG16 (1:1,000; Abcam), rabbit anti-K8.1 (1:10,000), and rabbit anti-ORF59 (1:10,000). Rabbit anti-ORF59 and anti-K8.1 were produced by the Pocono Rabbit Farm and Laboratory by immunizing rabbits against MBP-ORF59 or MBP-K8.1 (gifts from Denise Whitby [30]). Following incubation with primary antibodies, the membranes were washed with TBST and incubated with the appropriate secondary antibody. The secondary antibodies used were the following: goat anti-mouse-HRP (1:5,000; Southern Biotech) and goat anti-rabbit-HRP (1:5,000; Southern Biotech).

The co-IP efficiency for the pairwise interactions was quantified from the Western blot images using Image Lab software (Bio-Rad). The band intensities for both the Strep-tagged ORF and ORF18^{WT}-3×FLAG or the mutant ORF18 (ORF18^{Mu}-3×FLAG) were calculated for the IP lanes of the Western blots. The ratio

TABLE 1 Primer sequences used in this study

Primer no.	Target or purpose	Sequence 5′–3′	Orientation[a]
1	ORF18 (L29A)	CATGTGGCGCTTTTTGCAAAATAAGAATGCAAATACATTCCACGCCCAAG	F
2	ORF18 (L29A)	CTTGGGCGTGGAATGTATTTGCATTCTTATTTTGCAAAAAGCGCCACATG	R
3	ORF18 (E36A)	AATACATTCCACGCCCAAGCGCTGCGTTTTATTCATTTG	F
4	ORF18 (E36A)	CAAATGAATAAAACGCAGCGCTTGGGCGTGGAATGTATT	R
5	ORF18 (L37A)	GAACCAAATGAATAAAACGCGCCTCTTGGGCGTGGAATGTAT	F
6	ORF18 (L37A)	ATACATTCCACGCCCAAGAGGCGCGTTTTATTCATTTGGTTC	R
7	ORF18 (N63A)	GGGAGGCTACTGCCGCTGCCGGGACCTACG	F
8	ORF18 (N63A)	CGTAGGTCCCGGCAGCGGCAGTAGCCTCCC	R
9	ORF18 (G65A)	CTCGTCGTAGGTCGCGGCATTGGCAGT	F
10	ORF18 (G65A)	ACTGCCAATGCCGCGACCTACGACGAG	R
11	ORF18 (L72A)	GAACCTTGCGTCCCGCGACCACCTCGTCGT	F
12	ORF18 (L72A)	ACGACGAGGTGGTCGCGGGACGCAAGGTTC	R
13	ORF18 (R74A)	CGCAGGAACCTTGGCTCCCAGGACCACC	F
14	ORF18 (R74A)	GGTGGTCCTGGGAGCCAAGGTTCCTGCG	R
15	ORF18 (K75A)	GGTCCTGGGACGCGCGGTTCCTGCGGAG	F
16	ORF18 (K75A)	CTCCGCAGGAACCGCGCGTCCCAGGACC	R
17	ORF18 (W81A)	TCGTACACGAGCTTCGCCACCTCCGCAGGAAC	F
18	ORF18 (W81A)	GTTCCTGCGGAGGTGGCGAAGCTCGTGTACGA	R
19	ORF18 (Y85A)	TCCTCGAGCCCATCGGCCACGAGCTTCCACAC	F
20	ORF18 (Y85A)	GTGTGGAAGCTCGTGGCCGATGGGCTCGAGGA	R
21	ORF18 (L107A)	GTTCAAGTGCATCCAGGCGCTGTCCCGGTATGCC	F
22	ORF18 (L107A)	GGCATACCGGGACAGCGCCTGGATGCACTTGAAC	R
23	ORF18 (G130A)	GTCGTGGGTGACCGCTAGCCGGTGAAA	F
24	ORF18 (G130A)	TTTCACCGGCTAGCGGTCACCCACGAC	R
25	ORF18 (G145A)	CAGATTAAACAAAAAGTTTGCGTCCACCAGGTTTTCCG	F
26	ORF18 (G145A)	CGGAAAACCTGGTGGACGCAAACTTTTTGTTTAATCTG	R
27	ORF18 (N146A)	TTCCCAGATTAAACAAAAAGGCTCCGTCCACCAGGTTTTCCG	F
28	ORF18 (N146A)	CGGAAAACCTGGTGGACGGAGCCTTTTTGTTTAATCTGGGAA	R
29	ORF18 (L151A)	GAGCACACTTCCCGCATTAAACAAAAAGTTTCCGTCCACC	F
30	ORF18 (L151A)	GGTGGACGGAAACTTTTTGTTTAATGCGGGAAGTGTGCTC	R
31	ORF18 (G152A)	TGCAGGGGAGCACACTTGCCAGATTAAACAAAAAG	F
32	ORF18 (G152A)	CTTTTTGTTTAATCTGGCAAGTGTGCTCCCCTGCA	R
33	ORF18 (R158A)	CGCAAGGAGCAGCGCGCAGGGGAGCACA	F
34	ORF18 (R158A)	TGTGCTCCCCTGCGCGCTGCTCCTTGCG	R
35	ORF18 (L159A)	CGCCGCAAGGAGCGCCCTGCAGGGGAGC	F
36	ORF18 (L159A)	GCTCCCCTGCAGGGCGCTCCTTGCGGCG	R
37	ORF18 (W170A)	ATCGCTGCCCGCAAAGGCGAGGCAGTAGCCC	F
38	ORF18 (W170A)	GGGCTACTGCCTCGCCTTTGCGGGCAGCGAT	R
39	ORF18 (G171A)	CGTGTTCATCGCTGGCCCAAAAGGCGAGG	F
40	ORF18 (G171A)	CCTCGCCTTTTGGGCCAGCGATGAACACG	R
41	ORF18 (E176A)	GCGCACCCAGCGTGCGTGTTCATCGCT	F
42	ORF18 (E176A)	AGCGATGAACACGCACGCTGGGTGCGC	R
43	ORF18 (R180A)	CTGGGCGAAGAAGGCCACCCAGCGTTCG	F
44	ORF18 (R180A)	CGAACGCTGGGTGGCCTTCTTCGCCCAG	R
45	ORF18 (L191A)	AAGACGCCCGGAGACTATCGCGTAGCAAATGAAAAGCTTC	F
46	ORF18 (L191A)	GAAGCTTTTCATTTGCTACGCGATAGTCTCCGGGCGTCTT	R
47	ORF18 (G214A)	CCTCCACCGGAGCGGGATAGCCC	F
48	ORF18 (G214A)	GGGCTATCCCGCTCCGGTGGAGG	R
49	ORF18 (G228A)	GCATACGTTCGTATGGCGTACATGGAGCGGA	F
50	ORF18 (G228A)	TCCGCTCCATGTACGCCATACGAACGTATGC	R
51	ORF18 (E36A_L37A)	CAGAGAACCAAATGAATAAAACGCGCCGCTTGGGCGTGGAATGTATTTAAAT	F
52	ORF18 (E36A_L37A)	ATTTAAATACATTCCACGCCCAAGCGGCGCGTTTTATTCATTTGGTTCTCTG	R
53	ORF18 (R74A_K75A)	CCTCCGCAGGAACCGCGGCTCCCAGGACCACCTCGTC	F
54	ORF18 (R74A_K75A)	GACGAGGTGGTCCTGGGAGCCGCGGTTCCTGCGGAGG	R
55	ORF18 (G145A_N146A)	CTTCCCAGATTAAACAAAAAGGCTGCGTCCACCAGGTTTTCCGGGG	F
56	ORF18 (G145A_N146A)	CCCCGGAAAACCTGGTGGACGCAGCCTTTTTGTTTAATCTGGGAAG	R
57	ORF18 (L151A_G152A)	AGGGGAGCACACTTGCCGCATTAAACAAAAAGTTTCCGTCCACCA	F
58	ORF18 (L151A_G152A)	TGGTGGACGGAAACTTTTTGTTTAATGCGGCAAGTGTGCTCCCCT	R
59	ORF18 (R158A_L159A)	CCGCCGCAAGGAGCGCCGCGCAGGGGAGCACAC	F
60	ORF18 (R158A_L159A)	GTGTGCTCCCCTGCGCGGCGCTCCTTGCGGCGG	R
61	ORF18 (W170A_G171A)	GTGTTCATCGCTGGCCGCAAAGGCGAGGCAGTAGCC	F
62	ORF18 (W170A_G171A)	GGCTACTGCCTCGCCTTTGCGGCCAGCGATGAACAC	R
63	pLVX-TetOneZeo	TTTTTGGAGGCCTAGGCTTTTGCAAAACGCGACCATGGCCAAGTTGACCAGTGC	F
64	pLVX-TetOneZeo	ATTGTTCCAGACGCGTTCAGTCCTGCTCCTCGGC	R
65	2xStrep-ORF34 pCDNA4	GAGAAGGGGGCGGCCTTTGCTTTGAGCTCGCTCGTGT	F
66	2xStrep-ORF34 pCDNA4	AAACGGGCCCTCTAGTTAGAGTTGGTTGAGTCCATTCTCCTTGATC	R
67	UL79-3xFLAG pCDNA4	TACCGAGCTCGGATCATGATGGCCCGCGACG	F
68	UL79-3xFLAG pCDNA4	CTCCCTCGAGCGGCCCCACGTCGTTAGCCAGCGT	R
69	UL91-2xStrep pCDNA4	TACCGAGCTCGGATCATGAACTCGTTGCTGGCGG	F
70	UL91-2xStrep pCDNA4	CTCCCTCGAGCGGCCCTGTCACAGGCGCCCGAG	R
71	ORF18^{WT} and ORF18^{E36_L37A} pLVX TetOneZeo	CCCTCGTAAAGAATTATGCTCGGAAAATACGTGTGTGAGACC	F
72	ORF18^{WT} and ORF18^{E36_L37A} pLVX TetOneZeo	GAGGTGGTCTGGATCTTAAACGGGCCCCTTGTCGTCG	R
73	UL79^{E48_L49A}-3xFLAG pCDNA4	ATGAGGCGTACGATCTTGGCTGCTTCCAAACGCAGCGAGC	F
74	UL79^{E48_L49A}-3xFLAG pCDNA4	GCTCGCTGCGTTTGGAAGCAGCCAAGATCGTACGCCTCAT	R

(Continued on next page)

TABLE 1 (Continued)

Primer no.	Target or purpose	Sequence 5′–3′	Orientation[a]
75	ORF59 promoter qPCR	AATCCACAGGCATGATTGC	F
76	ORF59 promoter qPCR	CACACTTCCACCTCCCCTAA	R
77	GAPDH promoter qPCR	TACTAGCGGTTTTACGGGCG	F
78	GAPDH promoter qPCR	TCGAACAGGAGGAGCAGAGACCGA	R

[a]F, forward; R, reverse.

of the band intensity of the Strep-tagged ORF to ORF18^{Mu}-3×FLAG was divided by the ratio of the Strep-tagged ORF to ORF18^{WT}-3×FLAG to generate a co-IP efficiency for each ORF18^{Mu} relative to the co-IP efficiency of ORF18^{WT}.

ORF30 protein stability. Translation was inhibited 24 h after transfection by the addition of 100 μg/ml cycloheximide for 0 to 8 h. Cells were washed once in cold PBS, and cell pellets were frozen until all samples were collected. The pellets were lysed in IP lysis buffer by rotation for 30 min at 4°C. Lysates were cleared by centrifugation at 21,000 × *g* for 10 min and then resolved by SDS-PAGE followed by Western blotting.

Virus characterization. For reactivation studies, 1×10^6 iSLK cells were plated in 10-cm dishes for 16 h and then induced with 1 μg/ml doxycycline and 1 mM sodium butyrate for an additional 72 h. To determine the DNA fold induction in reactivated cells, the cells were scraped and triturated in the induced medium, and 200 μl of the cell/supernatant suspension was treated overnight with 80 μg/ml proteinase K (Promega) in 1× proteinase K digestion buffer (10 mM Tris-HCl, pH 7.4, 100 mM NaCl, 1 mM EDTA, 0.5% SDS), after which DNA was extracted using a Quick-DNA Miniprep kit (Zymo). Viral DNA fold induction was quantified by qPCR using iTaq Universal SYBR Green Supermix (Bio-Rad) on a QuantStudio3 real-time PCR machine with primers 75/76 (Table 1) for the KSHV ORF59 promoter and normalized to the level of the GAPDH promoter with primers 77/78 (Table 1).

Infectious virion production was determined by supernatant transfer assay. Supernatant from induced iSLK cells was syringe filtered through a 0.45-μm-pore-size filter and diluted 1:2 with DMEM; then 2 ml of the supernatant was spinoculated onto 1×10^6 freshly trypsinized HEK293T cells for 2 h at 500 × *g*. After 24 h, the medium was aspirated, and the cells were washed once with cold PBS and cross-linked in 4% paraformaldehyde (PFA) (Ted Pella) diluted in PBS. The cells were pelleted and resuspended in PBS, and a minimum of 50,000 cells/sample were analyzed on a BD Accuri 6 flow cytometer. The data were analyzed using FlowJo (31).

Late gene reporter assay. HEK293T cells were plated in a six-well plate, and each well was transfected with 900 ng of DNA containing 125 ng each of pcDNA4 ORF18-3×FLAG or ORF18^{Mu}-3×FLAG, ORF24-2×Strep, ORF30-2×Strep, ORF31-2×Strep, 2×Strep-ORF34, ORF66-2×Strep and either K8.1 Pr pGL4.16 or ORF57 Pr pGL4.16, along with 25 ng of pRL-TK as an internal transfection control. To determine the basal promoter activity for the K8.1 and ORF57 promoters, HEK293T cells were transfected with 900 ng of DNA containing 125 ng of K8.1 Pr pGL4.16 or ORF57 Pr pGL4.16 along with 750 ng of empty pCDNA4 and 25 ng of pRL-TK. After 24 h, the cells were rinsed once with PBS, lysed by rocking for 15 min at room temperature in 500 μl of passive lysis buffer (Promega), and clarified by centrifugation at 21,000 × *g* for 2 min. Twenty microliters of the clarified lysate was added in triplicate to a white chimney well microplate (Greiner Bio-One) to measure luminescence on a Tecan M1000 microplate reader using a Dual-Luciferase Assay kit (Promega). The firefly luminescence was normalized to that of the internal *Renilla* luciferase control for each transfection.

ACKNOWLEDGMENTS

We thank all members of the Glaunsinger and Coscoy labs, in particular Matthew R. Gardner, for their helpful suggestions and critical readings of the manuscript.

This material is based upon work supported by the National Science Foundation Graduate Research Fellowship under grant number DGE 1752814 and a University of California, Berkeley, Chancellor's Fellowship awarded to A.F.C. B.A.G. is an investigator of the Howard Hughes Medical Institute. This research was also supported by NIH grant R01AI122528 to B.A.G.

REFERENCES

1. Li D, Fu W, Swaminathan S. 2018. Continuous DNA replication is required for late gene transcription and maintenance of replication compartments in gammaherpesviruses. PLoS Pathog 14:e1007070. https://doi.org/10.1371/journal.ppat.1007070.
2. Serio TR, Cahill N, Prout ME, Miller G. 1998. A functionally distinct TATA box required for late progression through the Epstein-Barr virus life cycle. J Virol 72:8338–8343.
3. Tang S, Yamanegi K, Zheng Z-M. 2004. Requirement of a 12-base-pair TATT-containing sequence and viral lytic DNA replication in activation of the Kaposi's sarcoma-associated herpesvirus K8.1 late promoter. J Virol 78:2609–2614. https://doi.org/10.1128/JVI.78.5.2609-2614.2004.
4. Wong-Ho E, Wu TT, Davis ZH, Zhang BQ, Huang J, Gong H, Deng HY, Liu FY, Glaunsinger B, Sun R. 2014. Unconventional sequence requirement for viral late gene core promoters of murine gammaherpesvirus 68. J Virol 88:3411–3422. https://doi.org/10.1128/JVI.01374-13.
5. Djavadian R, Hayes M, Johannsen E. 2018. CAGE-seq analysis of Epstein-Barr virus lytic gene transcription: 3 kinetic classes from 2 mechanisms. PLoS Pathog 14:e1007114. https://doi.org/10.1371/journal.ppat.1007114.

6. Gong D, Wu NC, Xie Y, Feng J, Tong L, Brulois KF, Luan H, Du Y, Jung JU, Wang C.-y, Kang MK, Park N-H, Sun R, Wu T-T. 2014. Kaposi's sarcoma-associated herpesvirus ORF18 and ORF30 are essential for late gene expression during lytic replication. J Virol 88:11369–11382. https://doi.org/10.1128/JVI.00793-14.
7. Nishimura M, Watanabe T, Yagi S, Yamanaka T, Fujimuro M. 2017. Kaposi's sarcoma-associated herpesvirus ORF34 is essential for late gene expression and virus production. Sci Rep 7:329. https://doi.org/10.1038/s41598-017-00401-7.
8. Davis ZH, Verschueren E, Jang GM, Kleffman K, Johnson JR, Park J, Shales M, Dollen J, Von Maher MC, Johnson T, Newton W, Ja S, Horner J, Hernandez RD, Krogan NJ, Glaunsinger BA. 2015. Global mapping of herpesvirus-host protein complexes reveals a transcription strategy for late genes. Mol Cell 57:349–360. https://doi.org/10.1016/j.molcel.2014.11.026.
9. Davis ZH, Hesser CR, Park J, Glaunsinger BA. 2016. Associated herpesvirus late gene transcription factor complex is essential for viral late gene expression. J Virol 90:599–604. https://doi.org/10.1128/JVI.02157-15.
10. Aubry V, Mure F, Mariame B, Deschamps T, Wyrwicz LS, Manet E, Gruffat H. 2014. Epstein-Barr virus late gene transcription depends on the assembly of a virus-specific preinitiation complex. J Virol 88:12825–12838. https://doi.org/10.1128/JVI.02139-14.
11. Wu T-T, Park T, Kim H, Tran T, Tong L, Martinez-Guzman D, Reyes N, Deng H, Sun R. 2009. ORF30 and ORF34 are essential for expression of late genes in murine gammaherpesvirus 68. J Virol 83:2265–2273. https://doi.org/10.1128/JVI.01785-08.
12. Arumugaswami V, Wu T-T, Martinez-Guzman D, Jia Q, Deng H, Reyes N, Sun R. 2006. ORF18 is a transfactor that is essential for late gene transcription of a gammaherpesvirus. J Virol 80:9730–9740. https://doi.org/10.1128/JVI.00246-06.
13. Jia Q, Wu T-T, Liao H-I, Chernishof V, Sun R. 2004. Murine gammaherpesvirus 68 open reading frame 31 is required for viral replication. J Virol 78:6610–6620. https://doi.org/10.1128/JVI.78.12.6610-6620.2004.
14. Brulois K, Wong L-Y, Lee H-R, Sivadas P, Ensser A, Feng P, Gao S-J, Toth Z, Jung JU. 2015. Association of Kaposi's sarcoma-associated herpesvirus ORF31 with ORF34 and ORF24 is critical for late gene expression. J Virol 89:6148–6154. https://doi.org/10.1128/JVI.00272-15.
15. Wong E, Wu T-T, Reyes N, Deng H, Sun R. 2007. Murine gammaherpesvirus 68 open reading frame 24 is required for late gene expression after DNA replication. J Virol 81:6761–6764. https://doi.org/10.1128/JVI.02726-06.
16. Gruffat H, Kadjouf F, Mariame B, Manet E. 2012. The Epstein-Barr virus BcRF1 gene product is a TBP-like protein with an essential role in late gene expression. J Virol 86:6023–6032. https://doi.org/10.1128/JVI.00159-12.
17. Wyrwicz LS, Rychlewski L. 2007. Identification of herpes TATT-binding protein. Antiviral Res 75:167–172. https://doi.org/10.1016/j.antiviral.2007.03.002.
18. Perng Y-C, Campbell JA, Lenschow DJ, Yu D. 2014. Human cytomegalovirus pUL79 is an elongation factor of RNA polymerase II for viral gene transcription. PLoS Pathog 10:e1004350. https://doi.org/10.1371/journal.ppat.1004350.
19. Pan D, Han T, Tang S, Xu W, Bao Q, Sun Y, Xuan B, Qian Z. 11 July 2018. Murine cytomegalovirus protein pM91 interacts with pM79 and is critical for viral late gene expression. J Virol . https://doi.org/10.1128/JVI.00675-18.
20. El-Guindy A, Lopez-Giraldez F, Delecluse HJ, McKenzie J, Miller G. 2014. A locus encompassing the Epstein-Barr virus bglf4 kinase regulates expression of genes encoding viral structural proteins. PLoS Pathog 10:e1004307. https://doi.org/10.1371/journal.ppat.1004307.
21. McKenzie J, Lopez-Giraldez F, Delecluse HJ, Walsh A, El-Guindy A. 2016. The Epstein-Barr virus immunoevasins BCRF1 and BPLF1 are expressed by a mechanism independent of the canonical late pre-initiation complex. PLoS Pathog 12:e1006008. https://doi.org/10.1371/journal.ppat.1006008.
22. Castañeda AF, Glaunsinger BA. 2018. The interaction between ORF18 and ORF30 is required for late gene expression in Kaposi's sarcoma-associated herpesvirus. bioRxiv https://doi.org/10.1101/401976.
23. Edgar RC. 2004. MUSCLE: multiple sequence alignment with high accuracy and high throughput. Nucleic Acids Res 32:1792–1797. https://doi.org/10.1093/nar/gkh340.
24. Brulois KF, Chang H, Lee a. S-Y, Ensser a, Wong L-Y, Toth Z, Lee SH, Lee H-R, Myoung J, Ganem D, Oh T-K, Kim JF, Gao S-J, Jung JU. 2012. Construction and manipulation of a new Kaposi's sarcoma-associated herpesvirus bacterial artificial chromosome clone. J Virol 86:9708–9720. https://doi.org/10.1128/JVI.01019-12.
25. Dill KA. 1985. Theory for the folding and stability of globular proteins. Biochemistry 24:1501–1509. https://doi.org/10.1021/bi00327a032.
26. White SH. 1992. Amino acid preferences of small proteins. J Mol Biol 227:991–995. https://doi.org/10.1016/0022-2836(92)90515-L.
27. Dixit PD, Maslov S. 2013. Evolutionary capacitance and control of protein stability in protein-protein interaction networks. PLoS Comput Biol 9:e1003023. https://doi.org/10.1371/journal.pcbi.1003023.
28. Avey D, Tepper S, Pifer B, Bahga A, Williams H, Gillen J, Li W, Ogden S, Zhu F. 2016. Discovery of a coregulatory interaction between Kaposi's sarcoma-associated herpesvirus ORF45 and the viral protein kinase ORF36. J Virol 90:5953–5964. https://doi.org/10.1128/JVI.00516-16.
29. Djavadian R, Chiu YF, Johannsen E. 2016. An Epstein-Barr virus-encoded protein complex requires an origin of lytic replication in cis to mediate late gene transcription. PLoS Pathog 12:e1005718. https://doi.org/10.1371/journal.ppat.1005718.
30. Labo N, Miley W, Marshall V, Gillette W, Esposito D, Bess M, Turano A, Uldrick T, Polizzotto MN, Wyvill KM, Bagni R, Yarchoan R, Whitby D. 2014. Heterogeneity and breadth of host antibody response to KSHV infection demonstrated by systematic analysis of the KSHV proteome. PLoS Pathog 10:e1004046. https://doi.org/10.1371/journal.ppat.1004046.
31. Gardner MR, Glaunsinger BA. 2018. Kaposi's sarcoma-associated herpesvirus ORF68 is a DNA binding protein required for viral genome cleavage and packaging. J Virol 92:e00840-18. https://doi.org/10.1128/JVI.00840-18.